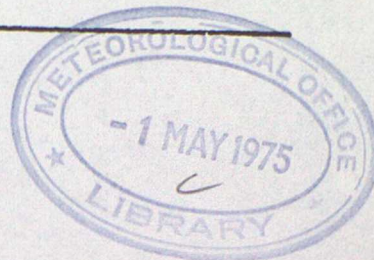


MET.O.14

METEOROLOGICAL OFFICE
BOUNDARY LAYER RESEARCH BRANCH
TURBULENCE & DIFFUSION NOTE



T.D.N. No. 61.

0119130

"THE STRUCTURE AND ENERGETICS OF A SUBSIDENCE INVERSION
PERTURBED BY A LEE-WAVE"

by

S.J.Caughey and C.J.Readings

April 1975

Please note: Permission to quote from this unpublished note should be
obtained from the Head of Met.O.14, Bracknell, Berks., U.K.

FH2

"THE STRUCTURE AND ENERGETICS OF A SUBSIDENCE INVERSION PERTURBED

BY A LEE-WAVE"

by

S.J. Caughey and C.J. Readings

1. Introduction.

The past few years have seen a growing awareness of the importance of the synoptic inversion in the diurnal development of the convective boundary layer. This has arisen partly because of some recent theoretical work (eg Ball (1960), Carson and Smith (1974), Tennekes (1973), Deardorff (1972) and Stull (1973)) and partly as a result of some recent experimental observations (eg Atlas et al (1970) and Rayment and Readings (1974)). Atlas et al (1970) used an FM/CW radar to study a maritime inversion and observed some complex structures including small scale billows and gravity waves (see Ottersen et al 1973). Some of these results were later confirmed by direct measurements from an aircraft (see Metcalf and Atlas (1973)). However it is not clear how applicable these observations are for example to the subsidence inversion commonly encountered over the British Isles. Some preliminary answers to this question were obtained during the experiment at Malvern, England in 1971 when a subsidence inversion was scanned by the high power 10 cm radar at Defford (see Watkins (1971)) at the same time as direct measurements were made in the vicinity of the actual interface by a turbulence probe mounted on the tethering cable of a kite balloon (see Browning et al (1973), Reading et al (1973) and Rayment and Readings (1974)). This revealed a hummocky interface with small scale billows on the crests of the hummocks (see figure 1). The entrainment rates deduced from this model were in close agreement with those derived from some radio sonde ascents. These observations also confirmed the importance of the entrained heat flux to the development of a convective boundary layer. However as only one inversion was studied, the general applicability of these results is not clear; thus further studies will have to be carried out before any general conclusions can be drawn. The present paper describes the results of just such a study. This revealed a different entrainment mechanism as well as providing further insight into the use of radio-sonde data for monitoring the development of a convective boundary layer.

2.

The observations described in this paper were made on 25 August 1972 near Malvern, Worcestershire (ie at the same site as the 1971 study); again using the Defford radar facility to monitor the overall structure of the atmosphere but this time direct measurements were made from the tethering cable of a balloon at three levels simultaneously. At each of these a Cardington turbulence probe (see Readings and Butler (1972)) was used to monitor the instantaneous values of (V , ϕ , T) - see glossary for an explanation of those and all the other symbols used in this paper. The outputs from these probes were relayed to the ground by radio telemetry and sampled once a second by a data logger. Although the radar observations were not as comprehensive as in 1971, because "dot angels" (probably caused by birds) prevented the Doppler facility being used, they still provide a fairly clear picture of the large scale features of the atmosphere. In addition, regular radio sonde ascents were made from Defford and a net radiometer was installed near the launch site.

On the day being considered there was a stationary anticyclone centred over the northern part of the British Isles and the early morning radio-sonde ascents from Defford revealed the presence of an inversion between 600-700 metres (see Figure 2). The radar observations showed that this inversion was distorted by a stationary lee wave as well as by hummocks (see Figure 3). However on this occasion the hummocks only lasted a few minutes and the development of the boundary layer was delayed by a layer of cloud which did not clear until just after midday (of Rayment and Readings 1974). This meant that no direct measurements were made before 1400Z; however after this time some 90 minutes of data were recorded by the three turbulence probes which were spaced at intervals of about 10 metres in the vertical. During the first hour these instruments were positioned at the interface of the inversion. This enabled the detailed structure of the surface to be studied and an entrainment model to be proposed, which is quite different from that previously described by Rayment and Readings (1974). The form of the spectra/cospectra is also described and the heat fluxes

derived from the WT-cospectra are compared with those calculated from the radio-sonde ascents (see section 3). This section also includes a comparison between the observed values of the inversion's height and those derived from the various 'rate equations' (see for example Deardorff (1973)). The final section is devoted to a discussion of all the results, including a comparison with those from the 1971 study and a consideration of possible future developments.

2.1 Detailed structure of the inversion interface:-

During the period of observation the radar records showed that the inversion interface was distorted by a lee wave as well as by transitory hummocks (see Figure 3). This figure also illustrates the way the inversion rose with time and it is interesting that the major increase in height occurred on the downwind side of the wave crests (of course on shorter time scales the inversion rises and falls with the passage of hummocks). This encourages the idea that entrainment arose from the 'rolling up' of the hummocks themselves, rather than by small scale mixing at the crests of the hummocks as was observed in 1971 (see Rayment and Readings, 1974). However before considering how well the turbulence data support this hypothesis some examples which illustrate the self-consistency of this data will be presented.

During the period 1413-1414Z the three probes moved from a trough (and air typical of that above the synoptic inversion) to being within the inversion itself. This is clearly illustrated by the temperature contours derived from the T-measurements made by these instruments; see the middle diagram in figure 4. Perhaps the most notable feature of this figure is the way the wind flow follows the T contours, for example consider the high frequency ϕ traces (see upper part of Figure 4) between 1413 and 1413(30)Z. Those of probes 2 and 3 show small fluctuations until 1413(30)Z when they begin to enter the interface, whilst probe 1 reflects the presence of the temperature contour distortions near 1413(15)Z. This correspondence applies equally well to quite small scale features such as the tongue of cold air at 1413(35)Z or larger scale features

such as the hummocks themselves (see for example the low frequency ϕ traces in the lower part of Figure 4). Numerous other examples of this self-consistency are available from other parts of the recordings.

Although these observations were made in the area where the radar indicated that the synoptic inversion was rising, none of the features shown in Figure 4 gives any clear indication of the nature of the entrainment mechanism responsible for transferring warm air downwards through the interface. The small tongue of cold air at 1413(35)Z may have been an unstable feature (since the local Richardson number was negative) but there were no clear examples of the small scale breakdowns previously reported by Readings et al (1973) anywhere in the records. However an event observed between 1445(30) and 1447(20) does seem to provide a fairly unambiguous example of the 'roll-up' of a complete hummock similar to that proposed by Carson and Smith (1974) (see Figure 5). This shows a region of warm air (centred at 1446Z) coincident with a strong downdraught. At a slightly later time this warm air undercuts the cold air and there is a strong updrift in this region. This tongue of warm air had a horizontal extent of about 240 m which is compatible with the size of the hummocks themselves (~ 400 m) and considerably larger than the small scale features described previously by Readings et al (1973). Although this was the only clear example of the 'roll-up', hummocks were being continually advected past the probes and several of them may well have been about to collapse.

2.2 A model for the entrainment process:-

From the results presented in the previous section it seems reasonable to argue that the mechanism responsible for the rise of the inversion could have been the 'roll-up' of the hummocks themselves and the subsequent transfer of warm air into the convective boundary layer. Now the radar records show that this process only occurred on the downwind side of the lee wave crests where presumably the vorticity field had been tightened sufficiently. Thus it

appears that on this occasion there was a train of hummocks being continually advected along the surface of the inversion and that the tilt of the isentropic surfaces, associated with their passage over the crest of the lee wave, could have been sufficient to cause them to overturn (Figure 6 gives a schematic representation of this process). This process is in marked contrast with the mechanism observed during the 1971 study which involved the breakdown of small scale billows on the crests of the hummocks (see Figure 1 and Rayment and Readings (1974)). However the process observed here is very similar to that proposed by Carson and Smith (1974) since the hummocks may not necessarily require the presence of a lee wave to initiate 'roll-up' provided there is sufficient wind shear across the interface.

To estimate the entrainment velocity (ie rate of inversion rise) on the basis of this mechanism, consider a series of hummocks approaching a lee wave and suppose they begin to 'roll-up' at the crest (see Figure 6). Then the volume of air incorporated into the boundary layer per unit cross wind width per roll up will be approximately $L \times l$ (see Figure 6 for the specification of these parameters). If the frequency of arrival of hummocks is f then the rate of entrainment will be

$$(Ll) \times f \quad \text{m}^3 \text{ sec}^{-1}$$

Assuming this occurs on the downwind side of the lee wave crest then the total rate of rise of the inversion in this region will be

$$\left(\frac{Ll}{\mathcal{L}} \right) \times f \quad \text{m sec}^{-1} \quad \dots\dots\dots (1)$$

where \mathcal{L} is the extent of this region. It follows from Figure 5 that $l \sim 15 \text{ m}$ and $L \sim 240 \text{ m}$. The radar records show that $\mathcal{L} \sim 600 \text{ m}$ and the hummocks were observed to arrive at a rate of about one every five minutes. Substitution of these values into equation (1) gives a value for the entrainment velocity of about 70 m hr^{-1} (ie approximately 7 mb hr^{-1}). This result is in good agreement with that deduced directly from the time averaged radar record (ie about 7 mb hr^{-1}).

2.3 Spectral Analysis:-

The total period of observation was divided into four sections and a Fast Fourier transform (see Rayment (1972)) was used to derive the various power and co-spectra. These sections may be described as follows:-

Section (I) (1358-1415)g - probes in the region close to but below the interface with only one excursion into the inversion.

Section (II) (1415-1432)g - probes generally in the interfacial region with large fluctuations of all the measured quantities.

Section (III) (1432-1449)g - similar to (I) but without an excursion through the interface.

Section (IV) (1507-1541)g - probes below and remote from the interface.

The power spectra $nS_u(n)$, $nS_W(n)$ and $nS_T(n)$ for all three probes in period IV are reproduced in Figure (7) and it can be seen that:-

- (i) there is a high degree of consistency between the spectra from the three probes;
- (ii) at the high frequency end of the spectra neither $nS_T(n)$ or $nS_W(n)$ fall off as $n^{-2/3}$, $nS_T(n)$ being steeper ($\sim n^{-1}$) and $nS_W(n)$ less steep);
- (iii) there is a secondary peak in $nS_W(n)$ at about 8×10^{-2} Hz which may reflect the presence of a second input scale;
- (iv) $nS_u(n)$ exhibits less consistency at the low frequency end than the other spectra and though there is a $2/3$ region (at intermediate frequencies) above 10^{-1} Hz the slope is markedly less than this.

Generally speaking the spectral slopes (at the high frequency end of the spectra) for the other three periods were all less than $-2/3$. This probably reflects the generation of small scale mixing in the vicinity of the interface (cf Readings et al 1973). At the low frequency end the traverses of the interface produced several marked irregularities in the spectral slopes.

Figure 8 shows the cospectra for the fluxes $\overline{W'T'}$, $\overline{U'T'}$ and $\overline{U'W'}$ during section IV. These all exhibit major troughs/peaks near 2×10^{-2} Hz and 6×10^{-3} Hz (as do all the cospectra for sections I-III). However their interpretation is rather ambiguous, since a negative fluctuation in $W'T'$ could arise from warm air descending (ie entrainment) or cooler air rising and mixing with the slightly warmer air in the neighbourhood of the inversion. The other cospectra do not resolve this ambiguity but since both processes are associated with entrainment it is still possible to estimate the entrained heat flux from the \overline{WT} -cospectra and these values can be compared with these deduced from radiosonde data (see 3.1). In doing this contributions from the extreme low frequency end were ignored since they merely reflect the presence of low frequency trends which are only partially removed in the derivation of the spectra.

3. The Energetics of the Inversion:-

3.1. The Heat Fluxes:-

During the course of this study five successful radiosonde ascents were made from Defford (see Figure 2). These showed that the lowest levels of the atmosphere could be divided into four distinct regions:-

- a. a super adiabatic layer in the lowest few metres
- b. an adiabatic layer below the inversion (extending over the bulk of the boundary layer).
- c. the inversion
- and
- d. a stable region above it.

Although on this occasion the layer of cloud (see section 1) prevented any appreciable change in the temperature of the air below the inversion until after 1100 GMT, it can be seen from figure 9 that subsidence appears to have occurred before this. This feature was also observed in the 1971 study (Rayment and Readings, 1974) and though it is not yet understood, it may reflect the initial interaction of convective elements with the inversion. After 1100 GMT the air

below the inversion started to warm up and there was an appreciable increase in the inversion height as well as clear indications of entrainment (see Figure 2). It is unlikely that these changes were appreciably affected by any synoptic developments since the stationary anticyclone over the northern part of the British Isles was not developing and the synoptic charts indicated that there was no significant advection. However the presence of the lee wave (probably associated with the hills near Malvern) makes it unlikely that the observations at Malvern were typical of the whole country although its development appears to have been controlled by the local entrainment mechanism (ie it reflects the incorporation of warm air into the boundary layer of humpback roll-up).

From about 1100 GMT onwards the inversion rose at about 10 mb hr^{-1} (see Figure 9) which is in reasonable accord with both the radar observations and the value derived from the entrainment model (see section 2.2). It also fits in well with the humidity profiles which appear to confirm that entrainment must have occurred after 1100 GMT. (If this were not true the energy required to increase the total water content below the inversion would have had to be larger than the net radiation at the surface).

A further insight into the changes may be obtained by applying the formula

$$\frac{\partial}{\partial t} (\overline{w'\theta'}) = \frac{1}{f_g} \left(\frac{\partial \bar{\theta}}{\partial t} + \bar{w} \frac{\partial \bar{\theta}}{\partial h} \right)$$

to the radiosonde data with the assumption $\bar{w} = 0$. (See for example Cattle and Weston (1973)). The results of these integrations (using 5 mb slabs) are reproduced in Figure 10 and it can be seen that:-

- a. both the entrained and surface heat fluxes reached their maxima between 1100 and 1500 GMT,
- b. the surface fluxes were small before 1100 GMT,
- c. the fluxes tend to fall off linearly with height,
and
- d. entrainment started after 1100 GMT.

Figure 11 shows that these results are quite compatible with those obtained by other techniques. It can be seen that the $\overline{W'\Theta'}_s$ curve follows the trends in the R_N curve very well and that the values of $\overline{W'\Theta'}_i$ obtained from Figure 10 agree very closely with those obtained using Ball's (1960) formula:-

$$\overline{W'\Theta'}_i = - \frac{c_p}{g} \frac{\delta(P_s - P_i)}{\delta t} \Delta\Theta'$$

(again with the assumption $\bar{W} = 0$). The values of $\frac{\delta(P_s - P_i)}{\delta t}$ were taken from Figure 9 and those of $\Delta\Theta'$ (here $\Delta\Theta'$ is the temperature discontinuity between the two air masses involved in the mixing) from the turbulence probes measurements. In this instance $\Delta\Theta'$ was not equal to the strength of the synoptic inversion as was the case in 1971 (see Rayment and Readings, 1974). The degree of agreement between these two estimates of the entrained heat fluxes is very encouraging and serves to underline the feasibility of using radiosonde data to investigate the development of convective boundary layers. Over the period 1100-1500 GMT the average value of $\overline{W'\Theta'}_i / \overline{W'\Theta'}_s$ was 0.18 (see Table 2), which is in reasonable agreement with the values quoted by some other workers (eg Cattle and Weston (1973), Carson (1973) or Betts (1973)). Its variation during the course of the day is also illustrated by Figure 10 though the peak value of this ratio may well have been much larger than the plots show (cf Rayment and Readings (1974)).

The heat fluxes deduced from the radiosonde profiles may also be compared with those calculated from the WT - cospectra (see section 2.3). As explained there, it seems that only certain parts of these cospectra reflect the presence of entrainment - the low frequency values being contaminated by the probes traversing the actual interface. If these are removed by integrating the WT - cospectra above .005 Hz then the values listed in Table 1 will be obtained. These clearly illustrate the presence of a downward heat flux and it is evident that this flux tended to increase (in magnitude) the closer the probe was to the interface. The fluxes for section IV can be compared with those deduced from the

radiosonde ascents over the period 1459-1624 GMT and it can be seen that the two sets of values are quite compatible. The probe fluxes tend to be larger than the radiosonde values but $\overline{W\Theta}_1$ was decreasing with time over this period and the direct measurements were made during the first half of the integration period. This result is very encouraging as it provides further evidence of the reliability of the flux profiles derived from the radio sonde ascents as well as tending to confirm the interpretation of the co-spectra given in section 2.3.

3.2 The use of rate equations to predict the inversions rise:-

There have been several theoretical treatments of the development of the dry convective boundary layer capped by a stable layer (see Carson and Smith (1974) and Deardorff (1974)). In these the inversion is represented by a step discontinuity in potential temperature (Θ) at the height of the interface (ie at $z = z_1$) and the entrained heat flux $\overline{W\Theta}_1$ is written as a fraction, A , of the surface flux $\overline{W\Theta}_s$ ie

$$\overline{W\Theta}_1 = -A \overline{W\Theta}_s \quad 0 \leq A \leq 1$$

The differential equation which describes the evolution of the unstable layer, if there is zero mean vertical motion, is (see Carson 1973),

$$z_1 \frac{d}{dt} \left(\frac{d\Theta^+}{dz} z_1 \right) = \overline{W\Theta}_s - 2 \overline{W\Theta}_1 \quad \dots\dots\dots (2)$$

and although this is not explicitly dependent on A its derivation assumes that A is constant. With the assumption that $\frac{d\Theta^+}{dz}$ remains constant equation (2)

may be integrated to give z_1 as a function of time. Perhaps the major difficulty associated with the use of any rate equation is the choice of $\frac{d\Theta^+}{dz}$, since this can only be obtained by rather subjective means from radiosonde profiles. In all the calculations described here, a value midway between those corresponding to the very stable region immediately above the inversion and the less stable region remote from the interface has been used (ie $\frac{d\Theta^+}{dz} \sim 0.00015^\circ\text{C cm}^{-1}$).

The results of these calculations are listed in Table 2 and it can be seen that the inversion height is underestimated by about 15%.

An alternative equation which involves A explicitly is

$$\frac{dz_i^2}{dt} = \frac{2(1+2A) \overline{w'\theta'_s}}{\frac{d\theta^+}{dz}} \dots\dots\dots (3)$$

(see Carson, 1973). Using $A = 0.2$ the values obtained for the inversion height (see Table 2) are only marginally better than those derived from equation (2). However increasing A improves the agreement, the values obtained with $A = 0.4$ being only $\sim 5\%$ too low. Although advective changes on this day were regarded as small still the possibility remains that the air at 1400Z may always have been under clear sky conditions with consequently a higher A value. It is interesting to note that with this value of A equation (3) is approximately the same as that quoted by Deardorff (1974) ie

$$\frac{dz_i}{dt} = \frac{1.8 \overline{w'\theta'_s}}{\left(z_i \frac{d\theta^+}{dz} + \frac{g W_*^2}{g/\theta z_i} \right)} \dots\dots\dots (4)$$

as the second term in the denominator is small.

Discussion:-

Combining the information from the 1971 and 1972 studies it is probably correct to conclude that although the overturning of billows is responsible for the transfer of warm air downwards through an inversion, the scale on which this occurs varies from one occasion to another. An intensive series of high resolution (ie FM/CW) radar observations, preferably in conjunction with some direct measurements, would be needed to confirm this hypothesis. Such observations would probably also help to resolve some of the questions arising from the spectra/cospectra; such as the slope of the T spectra or the origin of the irregular features of the W-spectra.

The fluxes derived from radio-sonde ascents, using the method applied by Cattle and Weston (1973), are very encouraging since they agree well with the estimates obtained by other means (see Section 3). This is important since it raises the possibility of using only radio-sonde data to analyse the development

of the boundary layer. However it is important to remember that Ball's (1960) formula must be used with care since $\Delta\theta'$ is not always equal to the strength of the synoptic inversion as derived from a radiosonde ascent. It is also encouraging to note that it seems feasible to derive heat fluxes from direct measurements very close to the interface. However both this and the downward integration technique require further appraisal to establish the conditions under which they may be usefully applied. The use of rate equations to predict inversion rise also appears quite promising and obviously merits further consideration.

TABLE 1

The vertical heat fluxes derived from the probe measurements

Probe	Heights (metres)	Fluxes (mw/cm ²)		
		Section I (1358-1415 GMT)	Section II (1415-1432 GMT)	Section III (1432-1499 GMT)
1	714	- 1.7	- 2.5	- 1.1
2	723	- 4.3	- 6.7	- 2.2
3	732	- 6.2	- 9.1	- 7.3
Probe	Height (metres)	Section IV (1509-1544)		
1	805	- 0.2		
2	814	- 2.8		
3	823	- 2.9		

TABLE 2

A comparison between observed and calculated inversion heights

Time (GMT)	Actual Inversion Height (m)	Entrained flux $\frac{\text{flux}}{W\Theta_1}$ (cm sec ⁻¹)	Surface flux $\frac{\text{flux}}{W\Theta_s}$ (")	$\frac{W\Theta_i}{W\Theta_s}$ (A)	Calculated values	
					Using Equation (2)	Using Equation (3) A = 0.4
1109	575	- 2.1	13.5	.16	575	575
1209	-	- 3.7	18.9	.20	645	669
1309	-	- 3.9	20.2	.19	736	781
1409	-	- 2.9	18.0	.16	822	886
1459	975	- 1.9	15.9	.12	878	956
1559	-	- 1.0	13.6	.07	931	1025
1624	1115				948	1049

GLOSSARY

g	acceleration due gravity
l, L	height and length scales of the volume of air incorporated into the boundary layer per hummock roll-up (see Figure 6).
L	distance over which roll up process takes place (see Figure 6).
n	frequency (H_z).
u', w'	departures from the means of the total horizontal and vertical wind speeds respectively.
V	the magnitude of the total wind speed measured by the probe.
C_p	specific heat of dry air at constant pressure (1.005 J/ deg C)
p	pressure
f	frequency of arrival of hummocks
z, z_i	height and height of inversion base respectively.
R_N	net radiation at the surface.
$C_{xy}(u)$	cospectrum of the variables x and y
$S_x(u)$	power spectrum of the variable x
W_*	defined by $(g/\theta \overline{w\theta_s} z_i)^{1/3}$
T, T'	temperature and the departure from the mean temperature respectively.
t	time.
ρ	air density.
θ, θ'	potential temperature and departure from the mean potential temperature respectively.
$\Delta\theta'$	potential temperature difference of the air masses involved in entrainment.
$\frac{d\theta}{dz}^+$	potential temperature gradient above the inversion.
ϕ	inclination of the total wind vector to the horizontal plane.

REFERENCES

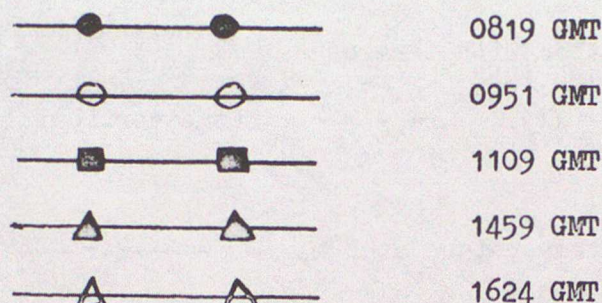
- ATLAS D., METCALF J.I., RICHTER J.H. and GOSSARD E.E. (1970) "The birth of CAT and microscale turbulence" *Journal of Atmospheric Sciences* 27 903-913.
- BALL F.K. (1960) "Control of inversion height by surface heating" *Quart. Journal of the Royal Met Soc* 86 483-494.
- BETTS A.K. (1973) "Non-precipitating cumulus convection and its parameterization" *Quart. Journal of the Royal Met Soc* 99 178-196.
- BROWNING K.A., STARR J.R. and WHYMAN A.J. (1973) "The structure of an inversion above a convective boundary layer as observed using high-power pulsed Doppler radar" *Boundary Layer Met.* 4 91-111.
- CARSON D.J. (1973) "The development of a dry inversion-capped convectively unstable boundary layer" *Quart Journal of the Royal Met Soc* 99 450-467.
- CARSON D.J. and SMITH F.B. (1974) "Thermodynamic model for the development of a convectively unstable boundary layer". *Advances in Geophysics* Vol 18A 111-124.
- CATTLE H. and WESTON K.J. (1973) "The structure and development of the boundary layer over land". *Quart Journal of the Royal Met Soc* 99 767-768.
- DEARDORFF J.W. (1972) "Numerical investigation of neutral and unstable planetary boundary layers". *J. Atmos. Sciences* 29 91-115.
- DEARDORFF J.W. (1974) "Three-dimensional numerical study of the height and mean structure of a heated planetary boundary layer" *Boundary Layer Met.* 7 81-106.
- METCALF J.I. and ATLAS D. (1973) "Microscale ordered motions and atmospheric structure associated with thin echo layers in stably stratified zones" *Boundary Layer Met* 4 7-35.
- OTTERSTEN H., HARDY K.R. and LITTLE C.G. (1973) "Radar and sodar probing of waves and turbulence in statically stable clear-air layers" *Boundary Layer* 4 47-89.

- RAYMENT R (1972)
 "Introduction to the transform (FFT) in the production of spectra" Met. Mag. 99 261-270.
- RAYMENT R. and READINGS C.J. (1974)
 "A case study of the structure and energetics of an inversion" Quart Journal of the Royal Met Soc 100 221-233.
- READINGS C.J. and BUTLER H.E. (1972)
 "The measurement of turbulence from a capture balloon". Met.Mag. 101 286-298.
- READINGS, C.J., GOLTON E. and BROWNING K.A. (1973)
 "Fine scale structure and mixing within an inversion" Boundary Layer Met 4 275-287.
- STULL R.B. (1973)
 "Inversion rise model based on penetrative convection" Journal Atmos. Sciences 30 1092-1099.
- TENNIKES H. (1973)
 "A model for the dynamics of the inversion above a convective boundary layer" Journal Atmos. Sciences 30 558-567.
- WATKINS C.D. (1971)
 "High power radar for meteorological studies in clear air" Proc. I.E.E. 118 519-527.

LIST OF FIGURES

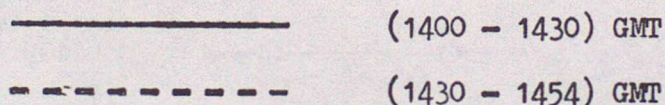
Figure 1:- A schematic model of the entrainment process observed during the 1971 Malvern study.

Figure 2:- Potential temperature (Θ) profiles from the Defford radio-sonde ascents on 25 August 1972.



Inset shows the 1323 GMT hodograph - hatched regions represent the location of the inversion; speeds are in m sec^{-1} and directions in $^{\circ}\text{N}$.

Figure 3:- The variation in the height of the radar echo from the inversion in both time and distance from the Defford site



These curves are averages of all the observations made over the periods stated. Hummocks were also observed but because of the short lifetimes do not appear on the average traces.

Figure 4:- Traces of the high and low frequency fluctuations of the wind inclination to the vertical (ϕ) and temperature contours constructed from the probes records. On the temperature contours the hatched regions correspond to regions above the inversion; on the ϕ records they are purely for clarification.

Figure 5:- Traces of the temperature contours and plots of the low frequency fluctuations - see caption to figure 4 for more detailed comments.

Figure 6:- Schematic representation of the entrainment mechanism observed during the 1972 study.

Figure 7:- Power spectra for each of the probes using the coding:-

●	Probe 3
X	" 2
△	" 1

Figure 8:- Cospectra for the three probes using the same coding as in Figure 7.

Figure 9:- The variation with time of

(a) $(h_s - h_i) - \text{---}$ (the vertical lines represent the confidence limits)

(b) the temperature at 8 m. - $\text{---} \times \times \times \text{---}$

(c) the mean potential temperature below the inversion

Figure 10 The successive $\overline{W\Theta}$ - profiles derived from the radio-sonde ascents at Defford:-

$\text{---} \bigcirc \text{---} \bigcirc \text{---}$	(0819 - 0951) GMT
$\text{---} \times \text{---} \times \text{---}$	(0951 - 1109) GMT
$\text{---} \bullet \text{---} \bullet \text{---}$	(1109 - 1459) GMT
---	(1459 - 1624) GMT

Figure 11 The variation of the surface and entrained heat fluxes and the net radiation with time:-

$\text{---} \bigcirc \text{---} \bigcirc \text{---}$	$\overline{W\Theta_i}$	from the $\overline{W\Theta}$ profiles.
$\text{---} \times \text{---} \times \text{---}$	$\overline{W\Theta_i}$	from $(\frac{dh}{dt})$ and $\Delta\Theta'$; the latter from the probe measurements.
$\text{---} \bullet \text{---} \bullet \text{---}$	$\overline{W\Theta_s}$	from the $\overline{W\Theta}$ profiles.
$\text{---} \square \text{---} \square \text{---}$	R_N	- net radiation.

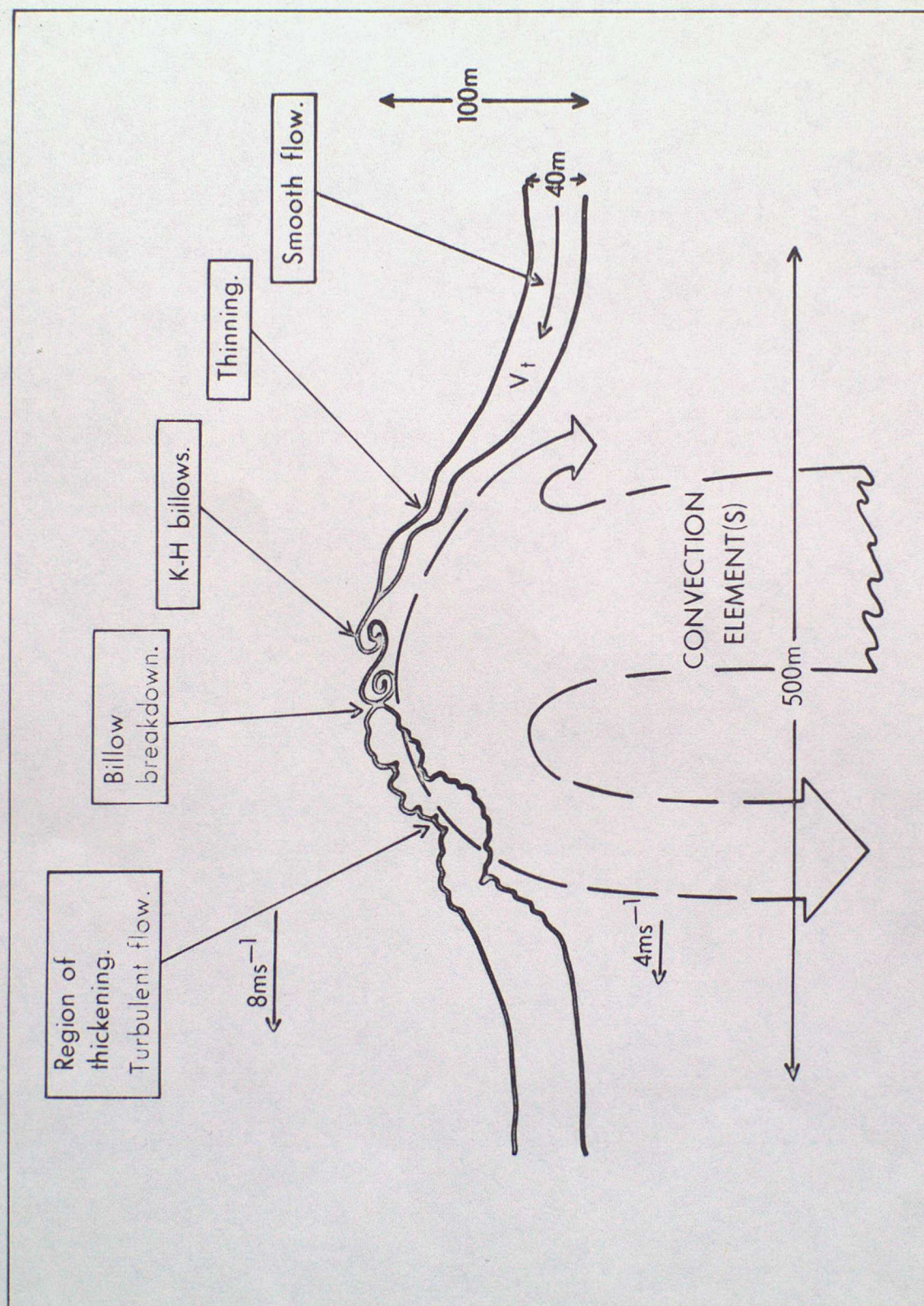


Figure 1

Figure 2

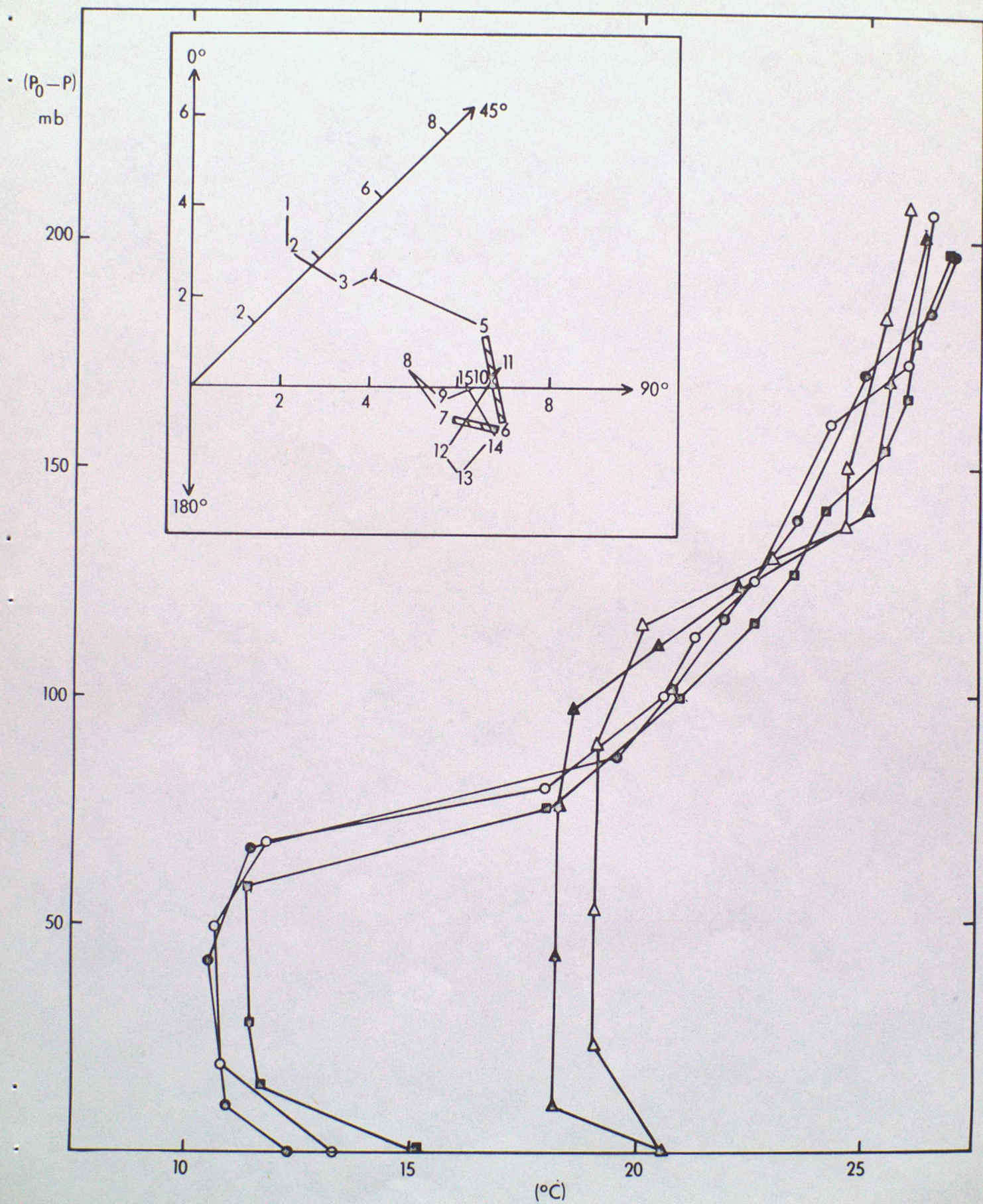


Figure 3

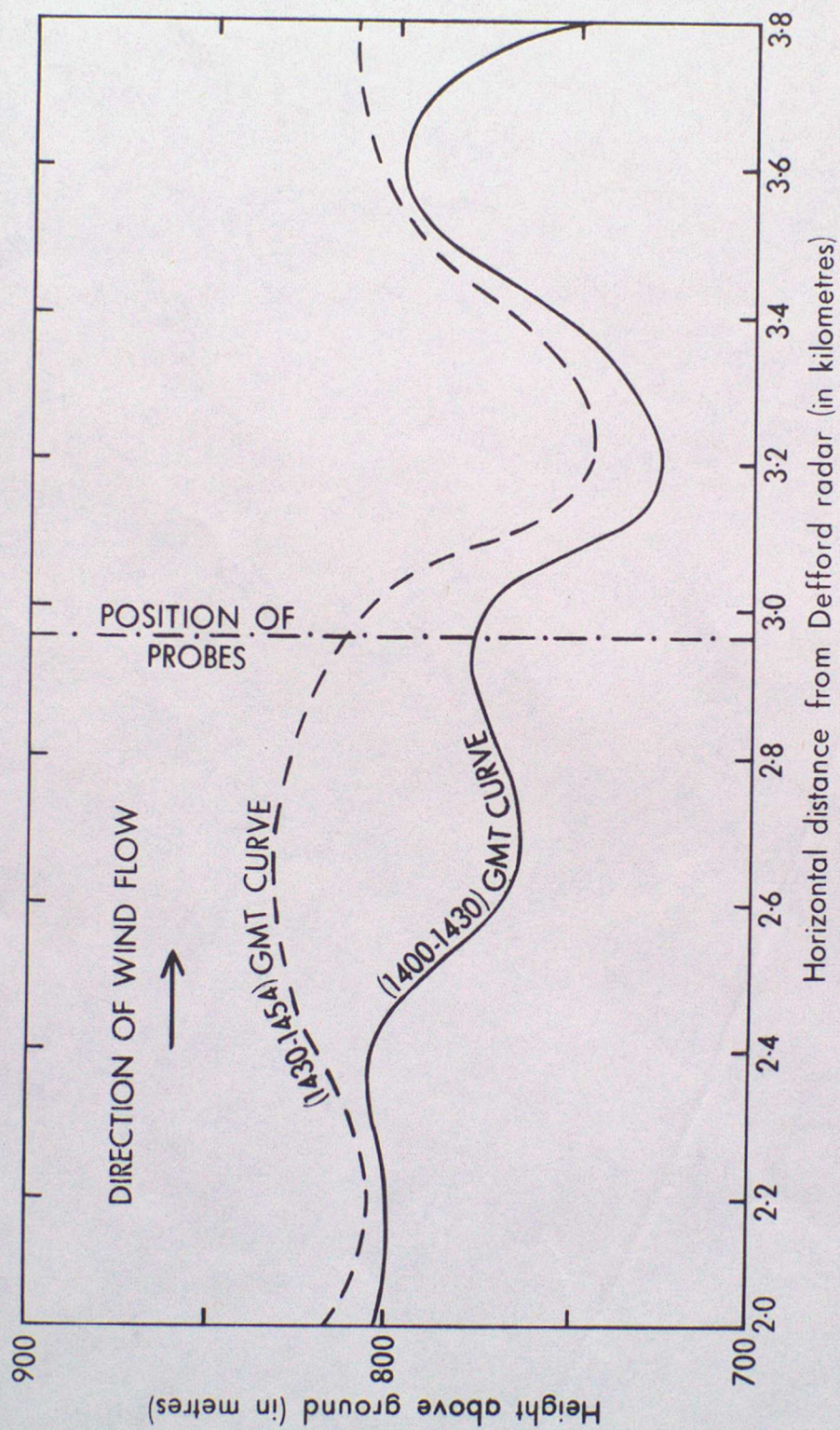


Figure 4

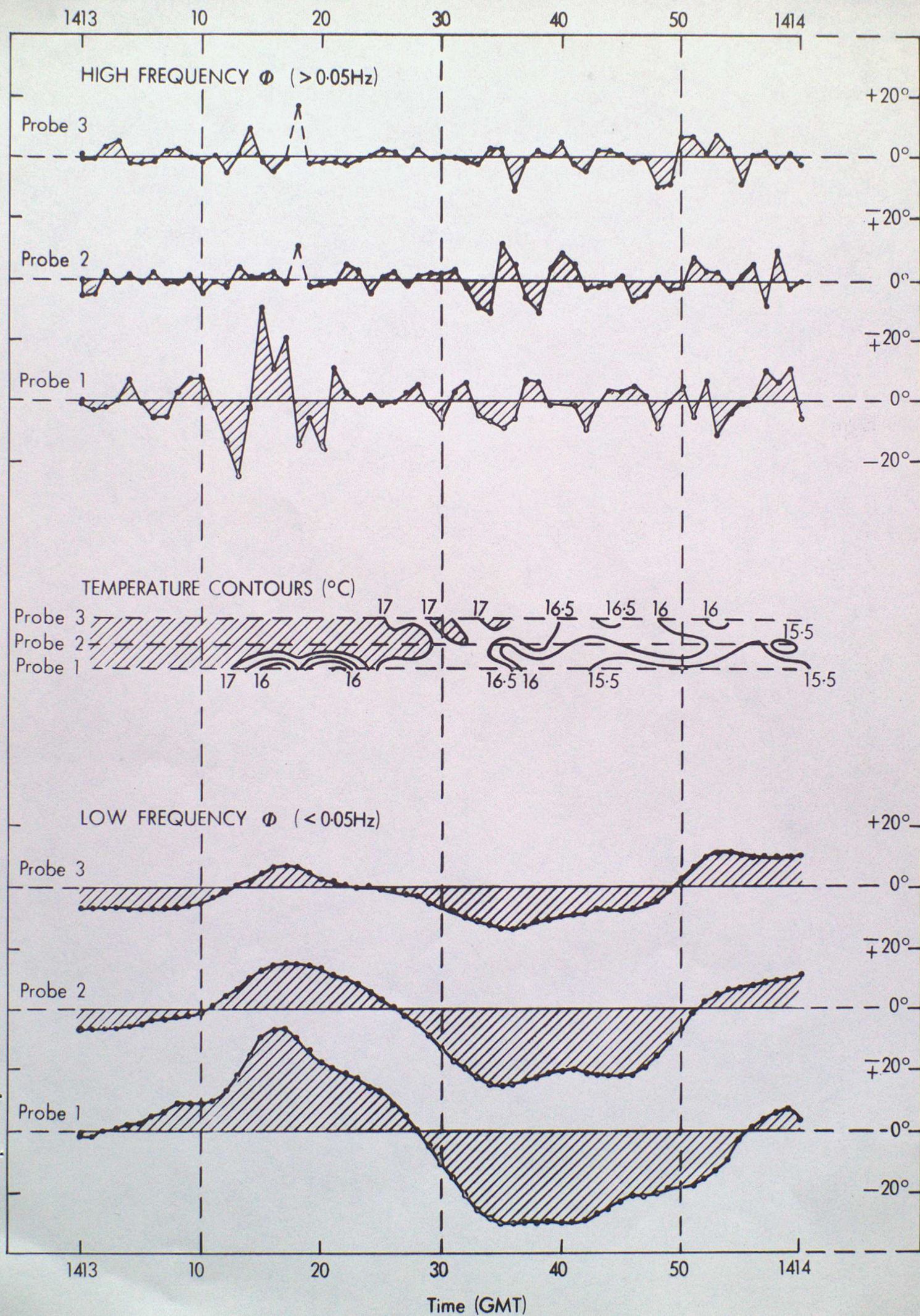


Figure 5

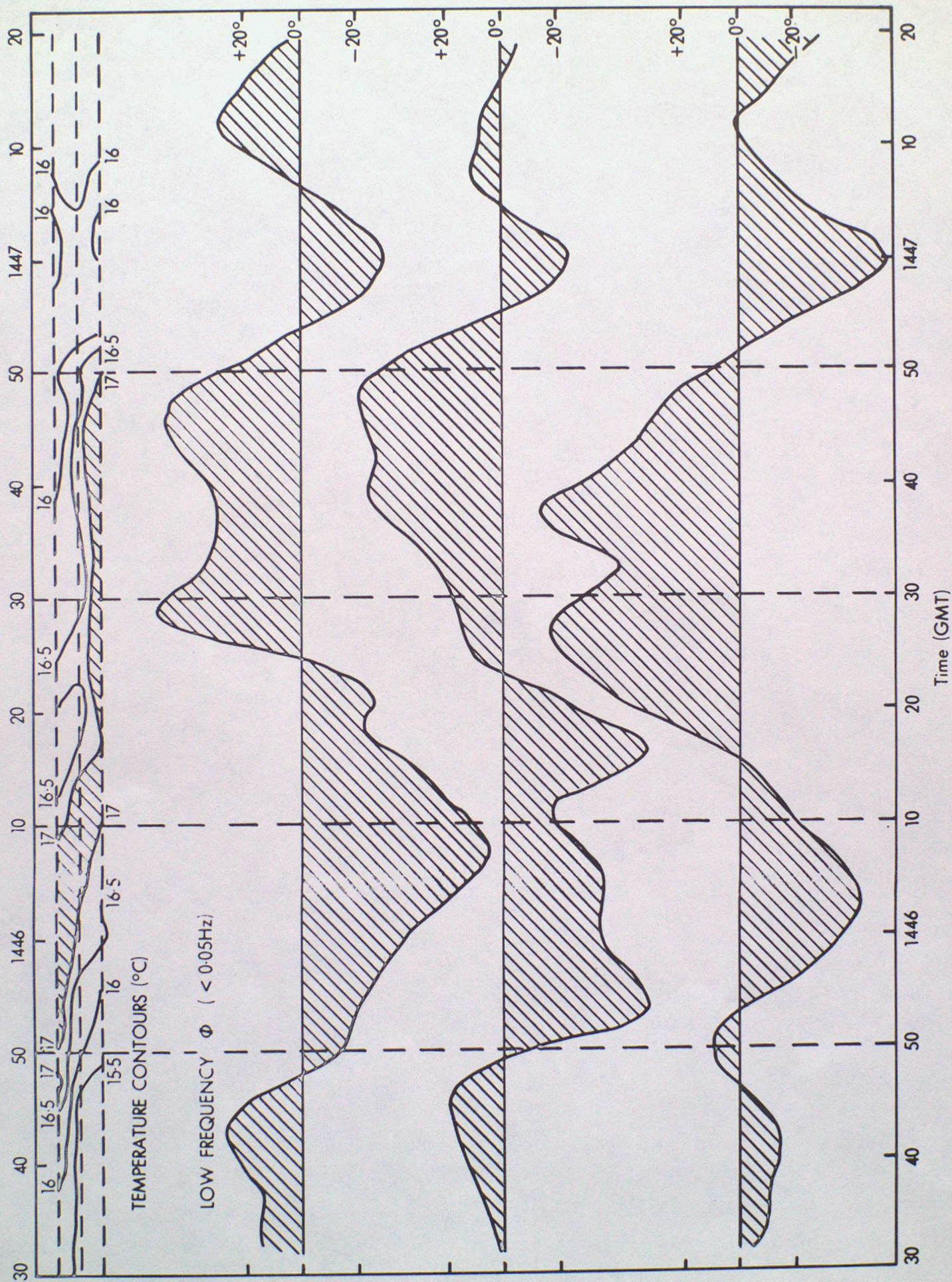


Figure 6

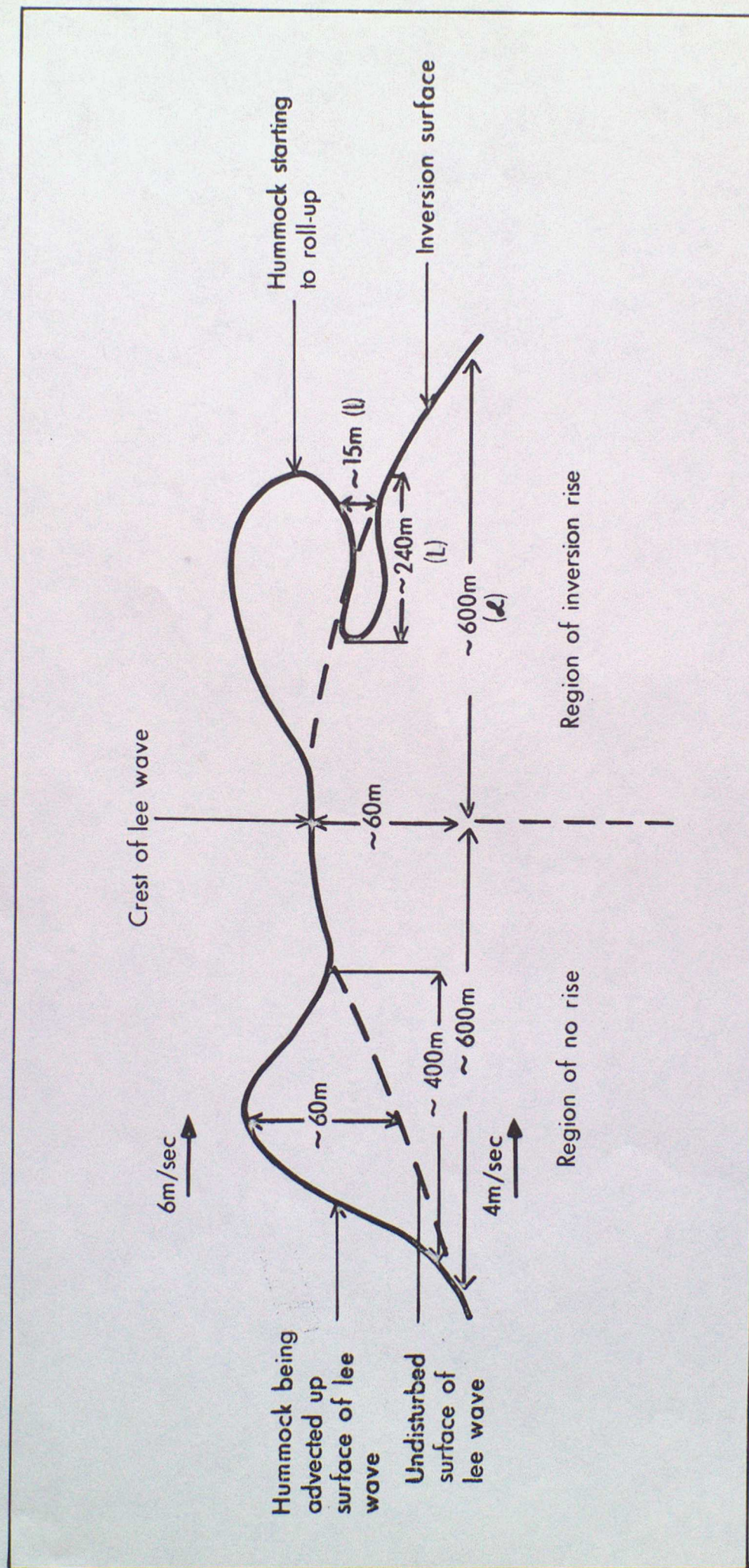


Figure 7

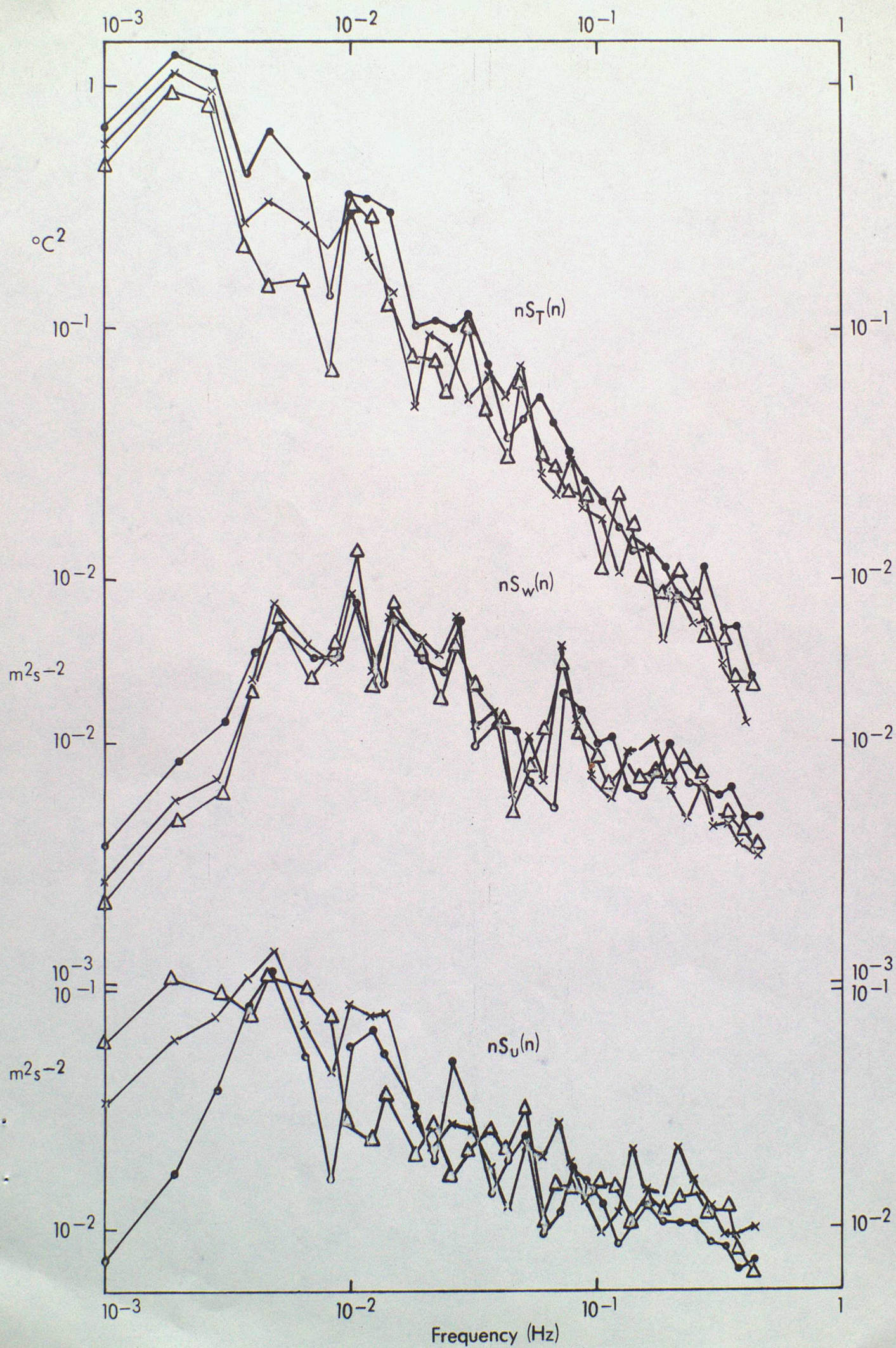
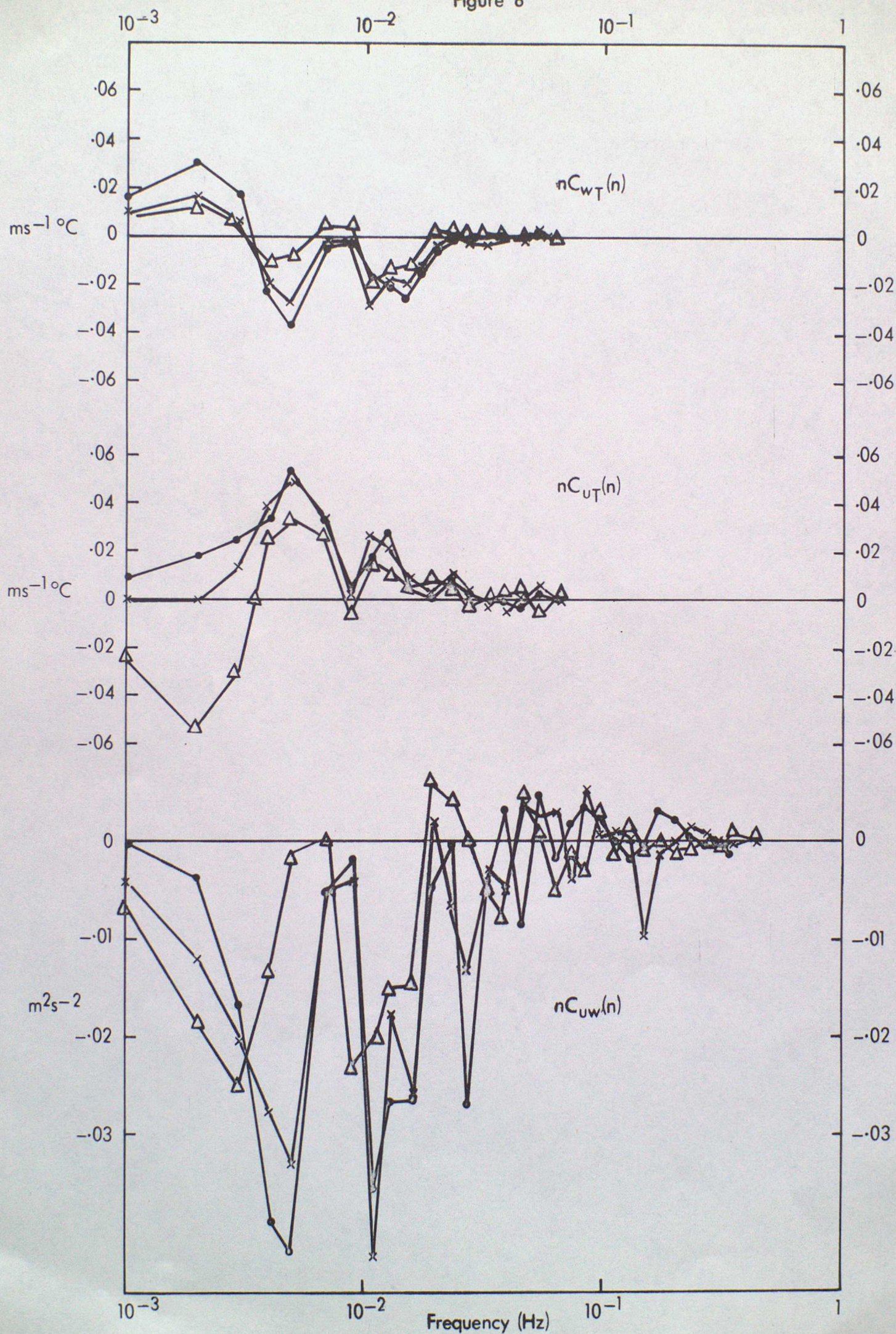


Figure 8



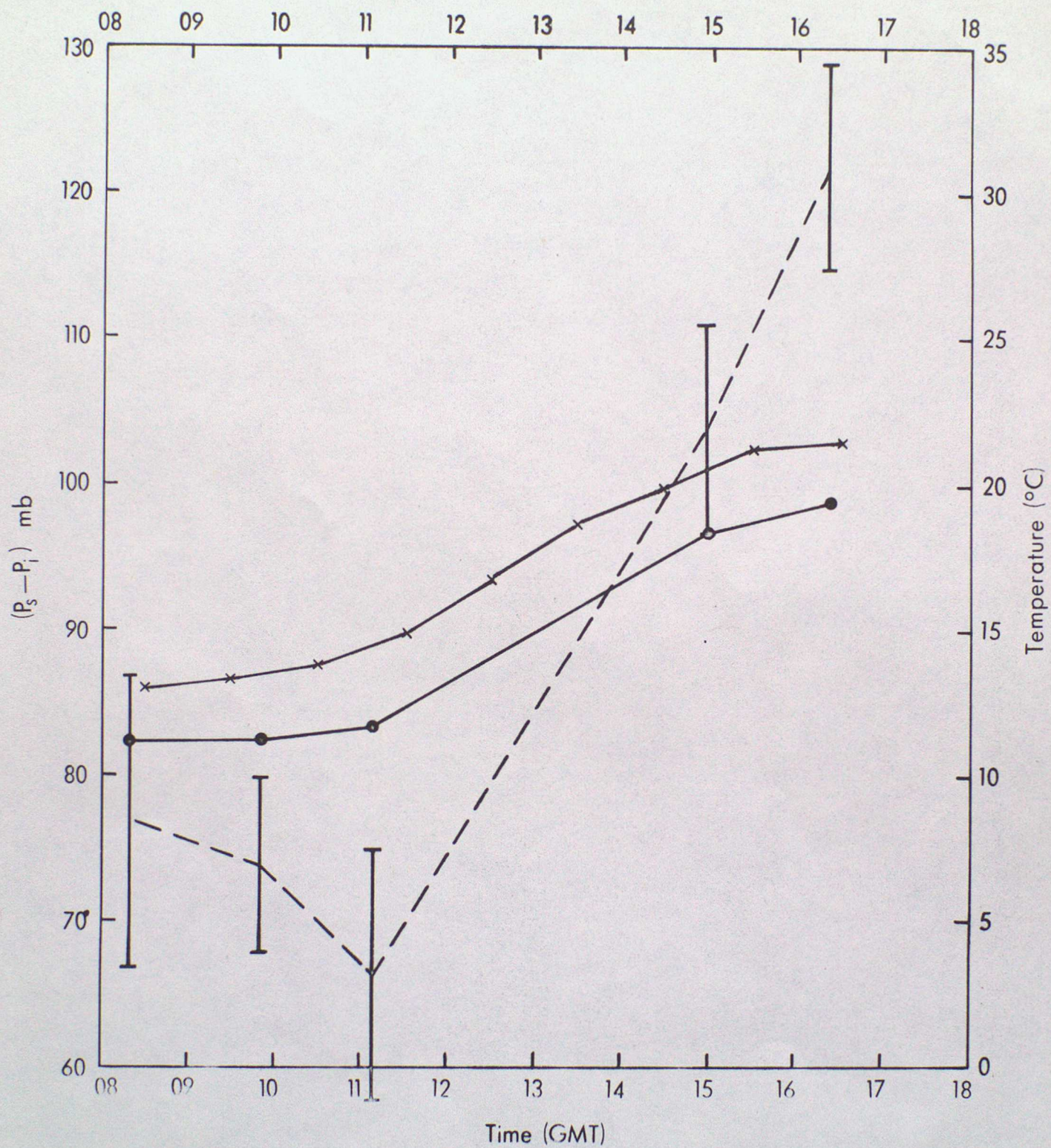
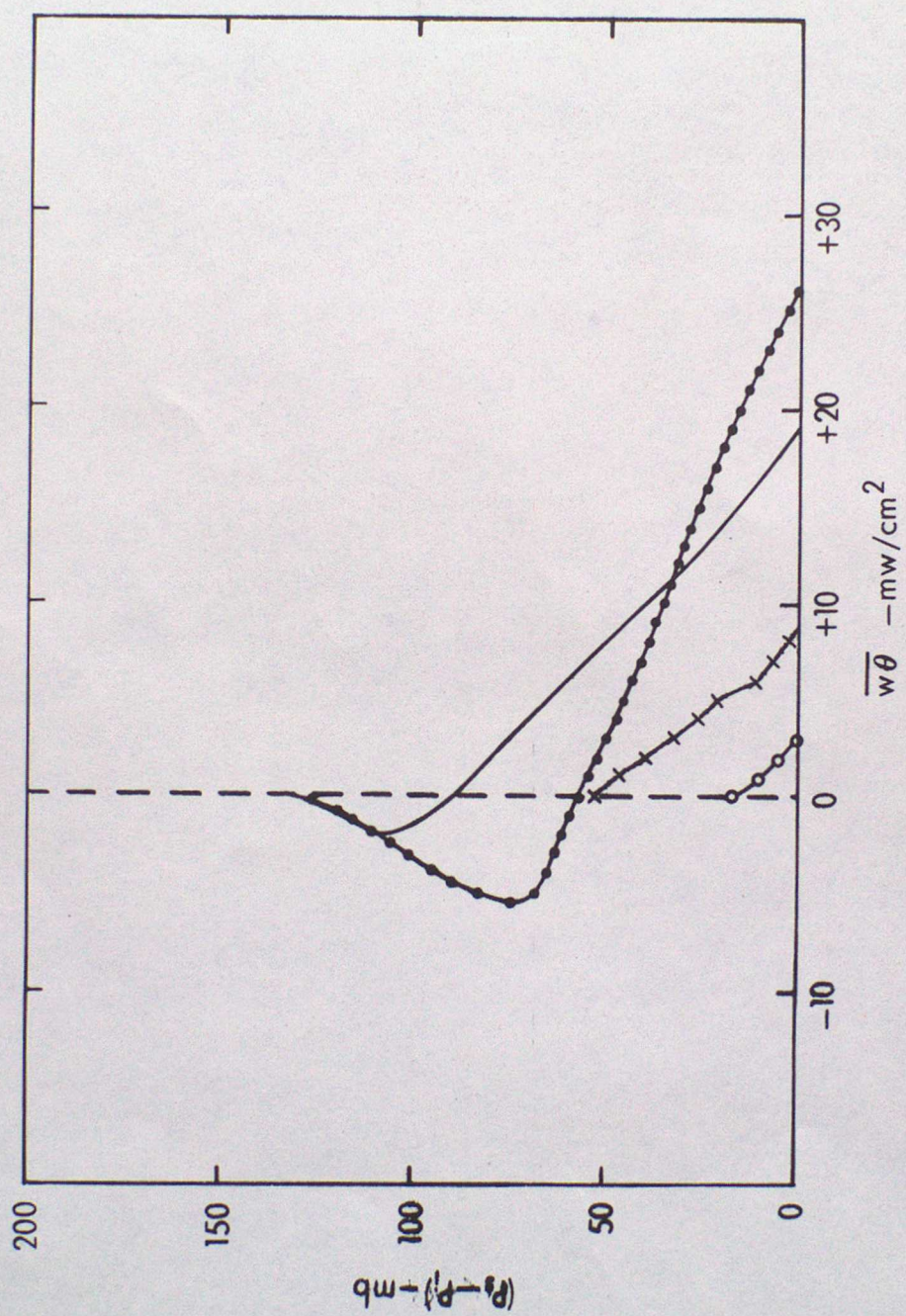


Figure 9

Figure 10



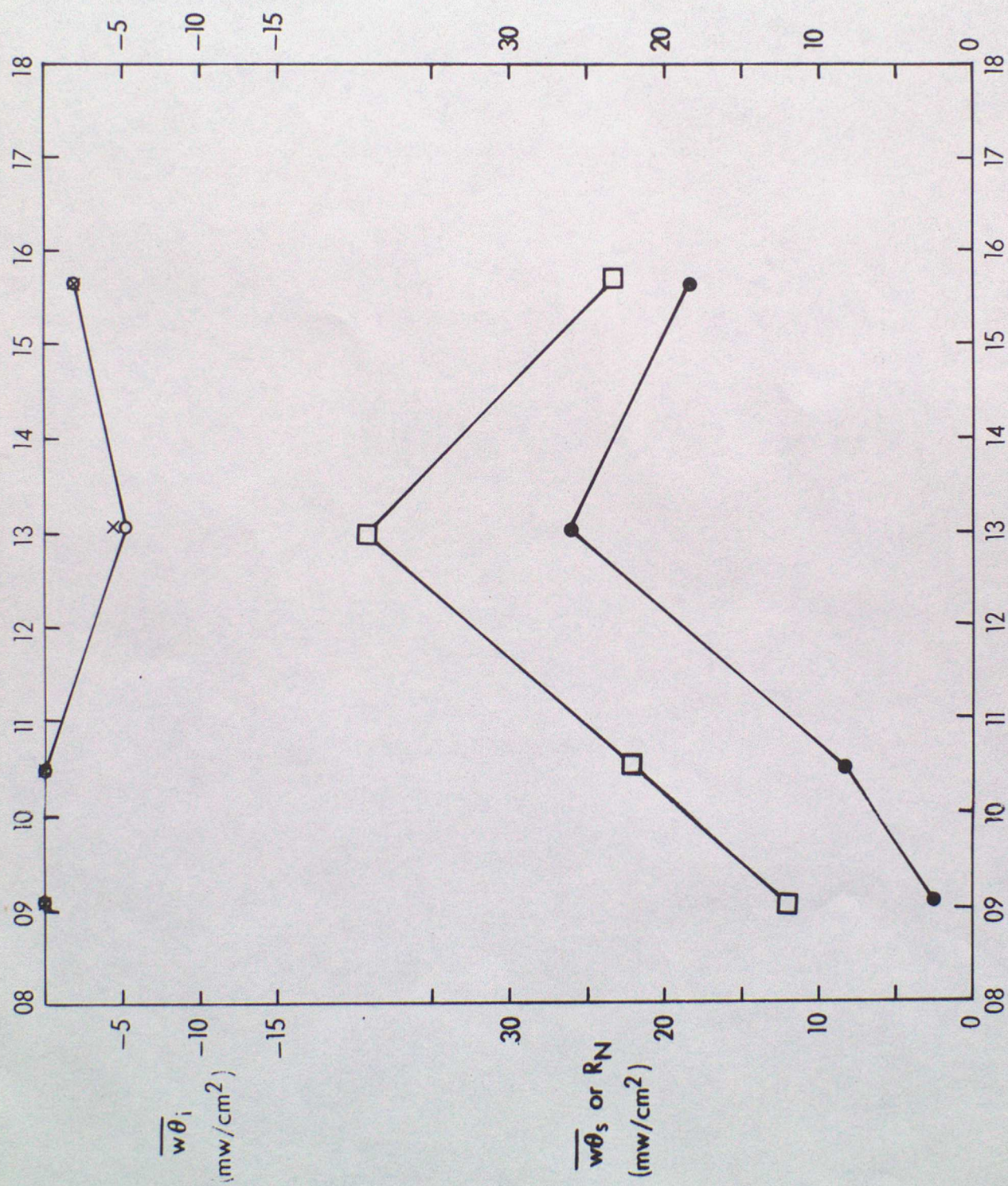


Figure 11